

SCIENTIFIC REPORTS



OPEN

Unravelling the spatial variation of nitrous oxide emissions from a step-feed plug-flow full scale wastewater treatment plant

Received: 06 October 2015
Accepted: 12 January 2016
Published: 08 February 2016

Yuting Pan^{1,4}, Ben van den Akker^{2,5,6}, Liu Ye^{1,3}, Bing-Jie Ni¹, Shane Watts¹, Katherine Reid² & Zhiguo Yuan¹

Plug-flow activated sludge reactors (ASR) that are step-feed with wastewater are widely adopted in wastewater treatment plants (WWTPs) due to their ability to maximise the use of the organic carbon in wastewater for denitrification. Nitrous oxide (N₂O) emissions are expected to vary along these reactors due to pronounced spatial variations in both biomass and substrate concentrations. However, to date, no detailed studies have characterised the impact of the step-feed configuration on emission variability. Here we report on the results from a comprehensive online N₂O monitoring campaign, which used multiple gas collection hoods to simultaneously measure emission along the length of a full-scale, step-feed, plug-flow ASR in Australia. The measured N₂O fluxes exhibited strong spatial-temporal variation along the reactor path. The step-feed configuration had a substantial influence on the N₂O emissions, where the N₂O emission factors in sections following the first and second step feed were $0.68\% \pm 0.09\%$ and $3.5\% \pm 0.49\%$ of the nitrogen load applied to each section. The relatively high biomass-specific nitrogen loading rate in the second section of the reactor was most likely cause of the high emissions from this section.

Nitrous oxide (N₂O) is a potent greenhouse gas (GHG), with an approximately 300-fold stronger global warming effect than carbon dioxide¹. In wastewater treatment plants, N₂O is mainly produced and emitted during biological nitrogen removal (BNR) process. The overall carbon footprint of a WWTP is highly sensitive to N₂O emission. For example, De Haas and Hartley² estimated that the carbon footprint of a WWTP would increase by approximately 30% if N₂O emission represented 1% of the nitrogen denitrified (or approximately 0.5% of the nitrogen load). Therefore, understanding N₂O emissions is of great importance to the operation of WWTPs, particularly as regulations are introduced to develop emission inventories and control strategies to reduce net environmental impacts.

In the past few years, there have been significant efforts worldwide to quantify and investigate N₂O emissions from full-scale BNR processes. The methods used have evolved from the initial grab-sampling based method³ to continuous online monitoring method, which has been now widely-adopted^{4,5}. The latter is typically done by monitoring the N₂O concentration and flow rate of gases over the operational range of the BNR process using portable online instruments. Many WWTPs are not enclosed and therefore floating hoods are often used to cover a small portion (e.g. 0.13 m²–0.6 m²) of the reactors surface to capture a representative gas sample^{4,6,7}. This approach is able to capture the diurnal and long-term temporal dynamics in the N₂O emission fluxes, which provides a more reliable means to quantify N₂O emissions.

¹Advanced Wastewater Management Centre, The University of Queensland, St. Lucia, QLD, Australia. ²Australian Water Quality Centre, Adelaide, 5000, South Australia, Australia. ³School of Chemical Engineering, The University of Queensland, St. Lucia, Brisbane, QLD, 4072, Australia. ⁴Department of Environmental Science and Engineering, School of Architecture and Environment, Sichuan University, Chengdu, Sichuan 610065, China. ⁵Health and Environment Group, School of the Environment, Flinders University, Bedford Park, 5042, South Australia, Australia. ⁶Centre for Water Management and Reuse, School of Natural and Built Environments, University of South Australia, Mawson Lakes, 5095, South Australia, Australia. Correspondence and requests for materials should be addressed to Z.Y. (email: zhiguo@awmc.uq.edu.au)

	Influent		Effluent	
	Range	Average (\pm standard deviation)	Range	Average (\pm standard deviation)
Chemical oxygen demand, COD (mg/L)	345–788	499 \pm 104	51–310	54 \pm 102
Biological oxygen demand, BOD (mg/L)	88–335	207 \pm 54	2–17	6 \pm 4
Total Kjeldahl nitrogen, TKN (mg/L)	45.5–78.8	64.0 \pm 6.5	2–10	3.3 \pm 1.6
Ammonium, NH ₄ ⁺ (mg N/L)	36.8–54.5	47.4 \pm 3.5	0–7	0.3 \pm 0.64
Nitrate, NO ₃ ⁻ (mg N/L)	0–0.85	0.18 \pm 0.13	5–19	12.1 \pm 5
Nitrite, NO ₂ ⁻ (mg N/L)	not detectable		0.009–0.19	0.05 \pm 0.05
Nitrous oxide, N ₂ O (mg N/L)	0–0.0026	0.0012 \pm 0.00075	0.0007–0.1984	0.045 \pm 0.054

Table 1. Influent and effluent characteristics of the two-step plug-flow BNR reactor studied.

Continuous online monitoring has revealed that N₂O emissions from wastewater treatment systems are highly dynamic^{8,9}. Variation in several factors are believed to influence emission dynamics, which include the nitrogen loading rate⁴, dissolved oxygen (DO)⁵ and nitrite concentrations⁶. It has further been reported that N₂O is primarily emitted from the aerated zones of a reactor¹⁰. This is attributed to the intensive stripping of N₂O as it is being produced¹⁰. In comparison, negligible emissions have been observed from non-aerated zones due to the lack of active stripping⁴. N₂O production during wastewater treatment is primarily biological, with nitrifying and denitrifying microorganisms the primary facilitators within the aerobic zone and anoxic zones respectively, with the dominant source of N₂O believed to be generated by ammonia-oxidising microorganisms^{4,9}.

In addition to temporal fluctuations in N₂O emissions, strong spatial variation in emission has been previously reported; particularly for large plug-flow reactors given steep spatial gradients in concentrations of DO and nitrogen species can exist along the reactors path^{4,5,7,11}. These spatial variations in nitrogen and oxygen concentrations are highest plug flow reactors that are step-fed, whereby organic rich wastewater is re-introduced at a second stage to drive denitrification¹². However, in addition to spatial gradients in substrate concentrations the step-feed strategy also produces a gradient of biomass along the length of the reactor given the returned activated sludge (RAS) stream is typically fed only to the beginning of the reactor. As a result the biomass concentration is higher in the upstream sections than compared with the downstream sections because the biomass becomes diluted by the second step-feed. This results in an uneven biomass-specific nitrogen loading along the reactor. It is possible that this gradient in biomass concentration would cause further spatial variations in the N₂O fluxes, given previous studies have shown that the biomass-specific nitrogen loading rate has a strong influence on N₂O production^{4,13}. However to date, the effect of such a feeding strategy on N₂O emission has not been reported.

The need to characterise spatial variability in emissions is required not only to better quantify the plants emission factor, but to understand the key drivers for N₂O production and identify control measures. This would require an online monitoring approach that can measure N₂O concentrations at multiple locations. Accordingly, the overall aim of this study was twofold: 1) to characterise the spatial variation of N₂O emissions from a full-scale plug-flow WWTP by developing a novel online method that can sequentially measure N₂O concentrations in the off-gas from multiple locations; and 2) to investigate the effect that a step-feed configuration ASR has on N₂O emissions. To this end, a comprehensive online monitoring program was undertaken to quantify N₂O emissions at multiple sampling locations positioned along the aerobic zones of a plug-flow step-fed reactor. To complement the online monitoring program, an intensive manual sampling campaign was conducted whereby hourly mixed liquor grab samples were taken from multiple locations across the reactors over a four day period (daytime only), for liquid-phase analysis of N₂O and other inorganic nitrogen species. Further, the ammonium and Total Kjeldahl Nitrogen (TKN) concentrations in the influent were also measured to calculate the N₂O emission factors for the different steps.

Results

Wastewater characteristics and plant performance. The characteristics of the ASRs influent and effluent during the 7-week monitoring period are shown in Table 1. The average TCOD and TKN removal efficiencies were around 90% and 75%, respectively. Non-biodegradable COD was the main form of organic matter in the effluent, with an average concentration of 48 mg/L. Nitrate was the main nitrogen product in the effluent, with an average concentration of 12 mg N/L. The effluent N₂O concentration was typically below 0.1 mg N/L, and was one order of magnitude higher than concentrations detected within the influent (Table 1).

Diurnal and spatial variation of N₂O emissions. The long-term online monitoring showed that the N₂O emissions were highly dynamic; however, a reoccurring diurnal pattern of N₂O emission profiles was evident across all locations. Figure 1 shows the diurnal N₂O emission profiles at all six monitored locations across the two steps. The profiles generally followed a pattern with an “N₂O emission valley” in the morning and an “N₂O emission peak” after 18:00 pm. This pattern roughly mirrored the diurnal pattern of the influent flow rate as shown in Figure S1 within the Supplementary Content.

A high level of spatial variability of N₂O fluxes was also clearly observed along the reactor. For the 1st step, N₂O emission was negligible at Location 2 (the very beginning of the aeration zone). This is contradictory to some previous observations that N₂O emission tended to increase within this transition zone^{6,14}. Considerable amount of N₂O emission was observed at Location 3 (25 meters from the beginning of the aeration zone), with the peak flux measured at 0.5 g N/(hour \times m²). The highest N₂O emission was observed at Location 4 (50 meters from the beginning of the aeration zone) with the peak flux measured at 1.2 g N/(hour \times m²). High N₂O emissions were

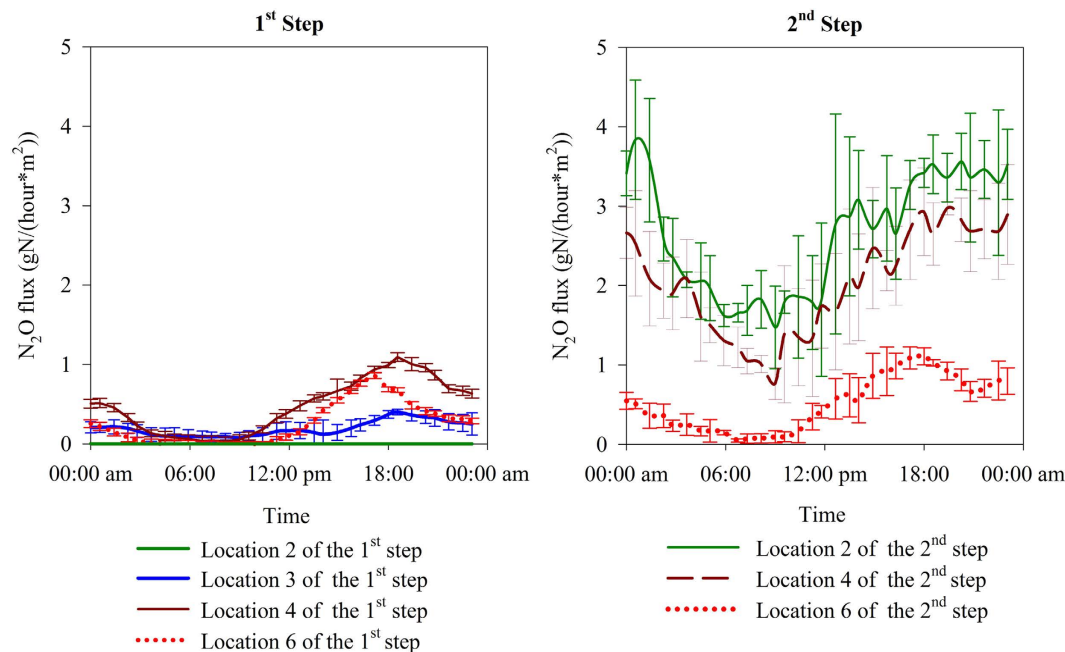


Figure 1. The average diurnal N_2O flux profiles from the 1st and the 2nd Step (error bars showing standard deviations).

also observed at the end of aeration zone of the 1st step (Location 6, which was 155 meters away from the beginning of the aeration zone), where the peak flux was $1.1 \text{ g N}/(\text{hour} \times \text{m}^2)$. However, the N_2O emission peaks from the middle of the aeration zone (Location 4) were much higher and wider than peaks from the end of the aeration zone (Location 6).

The spatial variation of N_2O fluxes from the 2nd step showed a different pattern in comparison to that of the 1st step. The highest N_2O emission was observed immediately after the anoxic zone (Location 2) with peak flux values measured around $4 \text{ g N}/(\text{hour} \times \text{m}^2)$. The N_2O emission flux reduced slightly at Location 4 (25 meters from the beginning of the aeration zone), and had reduced considerably at Location 6 (80 meters from the beginning of the aeration zone).

The N_2O fluxes measured within the 2nd step were significantly higher than the fluxes measured at the equivalent locations in the 1st step, particularly from the beginning and middle sections. At Locations 2 and 4 of the 2nd step, the N_2O fluxes were well above $1 \text{ g N}/(\text{hour} \times \text{m}^2)$ and typically reached $3.5 \text{ g N}/(\text{hour} \times \text{m}^2)$ for the majority of a day (>14 hours). In comparison, the N_2O emission fluxes at the equivalent locations along the 1st step were consistently lower than $1 \text{ g N}/(\text{hour} \times \text{m}^2)$.

Spatial variation of dissolved N_2O . Dissolved N_2O concentration in the influent was determined to be $0.0012 \pm 0.00075 \text{ mg N/L}$, which is within the previously reported ranges¹⁵. The dissolved N_2O concentration measured within the reactor (Fig. 2) was much higher than the N_2O concentration in the influent, which confirms that a significant amount of N_2O was produced during the BNR process. For each location, except for Location 2 of the 1st step, the dissolved N_2O concentration gradually increased from 8:00 am (when the manual sampling started) to 15:00 pm (when the manual sampling stopped). This ascending trend was in line with the gaseous N_2O emission trend shown in Fig. 1.

Similar to the online gaseous N_2O monitoring data, the spatial variability of dissolved N_2O concentration was substantial and the two steps display different patterns.

In the 1st step, negligible N_2O was found in the anoxic zone (Location 1) and at the beginning of the aeration zone (Location 2). This observation is consistent with the fact that no gaseous N_2O emission was observed at Location 2 of the 1st step (Fig. 1). The N_2O concentration gradually increased along the path of the plug-flow reactor of the 1st step. The highest N_2O concentrations were observed downstream at Locations 4, 5 and 6, where values ranged between 0.1 to 0.2 mg N/L at 3 pm.

Conversely, in the 2nd step, the dissolved N_2O concentration gradually reduced along the path of the plug-flow reactor. The highest N_2O concentration was observed in the anoxic zone (Location 1) and at the beginning of aeration zone (Location 2 and Location 3). The peak values at these locations were also observed at 3 pm, where values reached 0.4 to 0.5 mg N/L. The lowest dissolved N_2O concentration was observed at Location 6, which ranged between 0.06 and 0.19 mg N/L.

Overall, the dissolved N_2O concentration in the 2nd step was much higher than the 1st step, which was in line with the online gaseous N_2O emission profile.

Spatial variation of other parameters relevant to N_2O emissions. Several factors, such as DO level^{16–18}, nitrite or free nitrous acid (FNA) concentration^{19,20}, pH level^{21,22} have been shown to affect N_2O

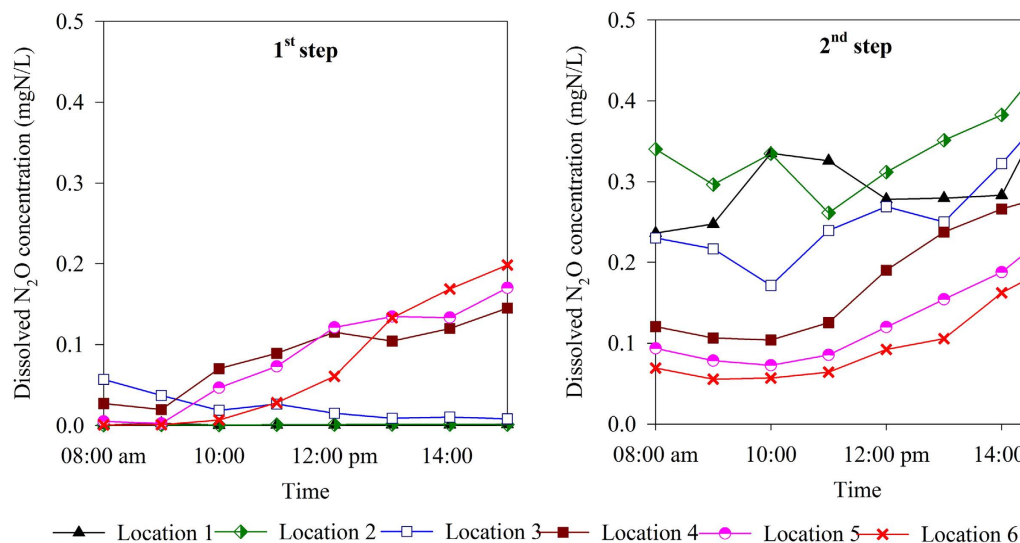


Figure 2. Liquid phase N_2O concentration in the 1st step and in the 2nd step.

production. Therefore, the spatial variations of these parameters, together with the NH_4^+ and NO_3^- concentrations, were monitored. The results are summarized in Fig. 3.

The spatial variation of NH_4^+ and NO_3^- concentrations seen here were expected for this type of reactor configuration. The NH_4^+ concentration gradually reduced from Location 2 to Location 6 in both steps (Fig. 3 a1 & b1), which was coupled with a gradual increase in the NO_3^- concentration due to nitrification (Fig. 3 a2 & b2).

The nitrite levels in the 1st step and in the 2nd step showed very different trends (Fig. 3 a3 & b3). In the 1st step, negligible NO_2^- was found in the anoxic zone (Location 1) and at the beginning of the aeration zone (Location 2). Higher NO_2^- concentrations (up to 0.35 mg N/L) were observed at downstream locations in the reactor (Locations 3, 4, 5 and 6). In contrast, the NO_2^- concentrations along the 2nd step gradually reduced along the path of the plug-flow reactor, with the highest NO_2^- concentration (up to 0.41 mg N/L) observed within the anoxic zone (Location 1) and at the beginning of aeration zone (Location 2).

The DO concentrations in the 1st and the 2nd steps showed very similar trends (Fig. 3 a4 & b4). Negligible DO concentration was detected in the anoxic zones (Location 1) of both steps. The DO concentration increased along the length of the aerobic zone (from locations 2 to 6) as COD and nitrogen substrates were oxidised and the aeration flow rate was kept steady. This ascending trend of DO along the reactor was more obvious in the morning (Location 6 of the 1st step and Locations 4, 5, 6 of the 2nd step), because the ammonium substrate was readily exhausted during this period of low loading (Fig. 3 b1).

Discussion

N_2O emission factor from the step-feed plug-flow system. To date, monitoring of many full-scale plants has been carried out with the awareness of N_2O as a potent greenhouse gas. Early investigations relied on the grab sampling method, which yielded highly variable N_2O emission factors with values ranging between 0.6% to 25% of the influent nitrogen load³. Due to the recent adoption of more reliable online monitoring methods, the N_2O emission factor has been refined and narrowed down greatly, with the reported emission factors for full-scale BNR plants varying between 0.01% to 6.8%^{4,5,7,11,23–25}. In this study, the combined N_2O emission factor of the two-step feed, plug-flow system was determined to be $1.9\% \pm 0.25\%$, which is among the highest values reported so far. For comparison, a literature review of reported N_2O emissions from full-scale wastewater treatment plants is shown Table S1 in Supplementary Content.

As shown in Fig. 1, significant temporal and spatial variability in the N_2O fluxes were observed along the plug-flow path. The calculated N_2O emission factor for each step, revealed that the step-feed configuration exerts a substantial influence on the N_2O emission, given that the N_2O emission factor from the first and second steps differed substantially, measuring $0.68\% \pm 0.09\%$ and $3.5\% \pm 0.49\%$, respectively, of the influent nitrogen loading to each path (Table 2). This result suggests that it is crucial to consider spatial variations of N_2O emission when quantifying emission factors from plug-flow systems.

For the majority of open reactors, characterising the spatial variability and emission ‘hotspots’ seen here presents a challenge, which was easily overcome by sequentially measuring N_2O concentrations in the off-gas from multiple hoods. Capturing this information was crucial to accurately quantify the reactors overall emission factor. Fully enclosed aeration basins would also benefit from this approach given the ability to identify hotspots and relate these with bulk water quality parameters can be used to identify the mechanisms responsible for N_2O production and hence allow more targeted performance optimisation measures to be made. This information would otherwise be missed if monitoring was focused solely on measuring the concentration of N_2O in the bulk off-gas from a common collection point.

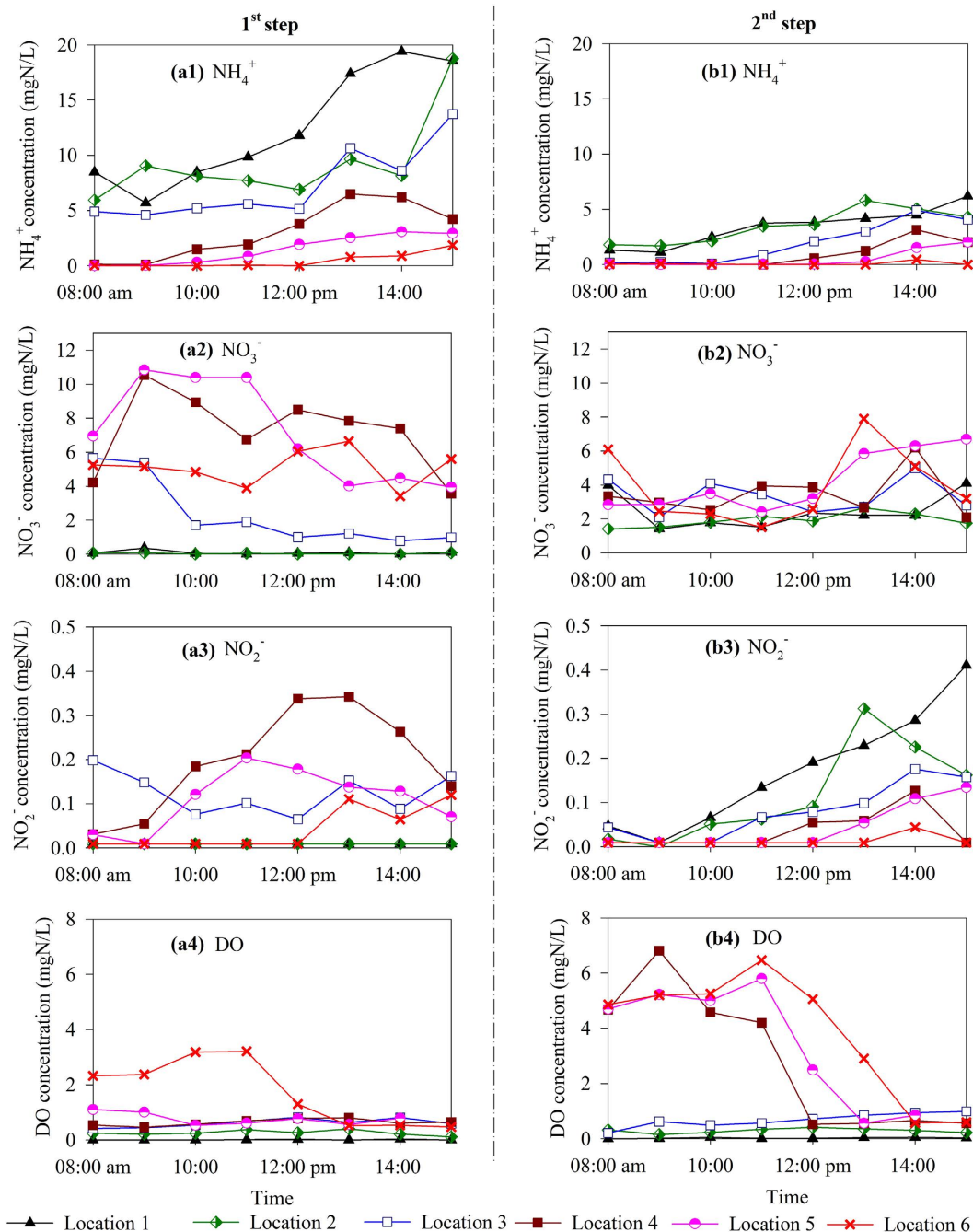


Figure 3. Liquid phase concentration profiles of NH_4^+ , NO_3^- , NO_2^- and DO in the 1st step and in the 2nd step.

	Average daily N_2O emitted (kg N/day)	Emission factor
Overall plant	62.3	$1.9\% \pm 0.25\%$
1 st step	12.5	$0.68\% \pm 0.09\%$
2 nd step	49.8	$3.5\% \pm 0.49\%$

Table 2. N_2O emissions determined for the two-step feed, plug-flow reactor.

Likely mechanism of N_2O emission variations in the step-feed plug-flow system. The major N_2O production pathways during BNR process include the hydroxylamine oxidation pathway of ammonia oxidizing bacteria (AOB), nitrifier denitrification pathway of AOB, heterotrophic denitrification pathway and chemical

reactions^{26,27}. The interplay of many parameters (such as DO and nitrite concentrations) determines the functional N₂O production pathways as well as the overall emission factor^{28,29}.

For the plant studied, the majority of N₂O that was emitted from the 1st step was generated in the aerobic zone, which was likely due to the nitrification process. This conclusion is based on the fact that there was negligible N₂O accumulation in the anoxic zone of the 1st step (Fig. 2) as well as negligible N₂O emission at the beginning of the aeration zone (Location 2) (Fig. 1). The negligible level of nitrate and nitrite at Location 1 (Fig. 3) showed that the anoxic zone in the 1st step was able to completely remove the small amount of oxidised nitrogen that was introduced by the RAS stream, which resulted in no N₂O accumulation from heterotrophic denitrification. Therefore, the anoxic zone of the 1st step played a very minor role in the overall N₂O emission factor.

In contrast to the 1st step, N₂O was generated in both the anoxic and aerobic zones of the 2nd step. N₂O accumulated to concentrations as high as 0.5 mg N/L at Location 1 in the anoxic zone of the 2nd step, indicating that there was N₂O accumulation during denitrification in the anoxic zone. The N₂O accumulated in the anoxic zone was subsequently stripped at the beginning of the following aerobic zone, which was captured by the hood located at Location 3. As shown in Fig. 3, in contrast to the negligible nitrate and nitrite concentrations in the anoxic zone in the 1st step, the nitrate and nitrite concentrations in the anoxic zone in the 2nd step reached 4.0 and 0.4 mg N/L respectively. This indicated that denitrification in the anoxic zone in the 2nd step was incomplete; a condition favouring N₂O accumulation³⁰. Denitrification was likely limited by the carbon source in the wastewater that was fed to this zone, resulting in N₂O accumulation.

This study revealed that the step-feed strategy could have a significant impact on N₂O emissions. The 2nd step had a much higher N₂O emission factor compared to the 1st step (Table 2) (3.5% vs. 0.68%). N₂O accumulation in the anoxic zone in the 2nd step clearly contributed to the higher emission factor. Based on the flow rate of the mixed liquor in the 2nd Step of 68.1 ML/day (27.3 + 22.7 + 18.1 = 68.1 ML/day, see section 2.1 for details), and the average dissolved N₂O concentration in the second anoxic zone of approximately 0.2 mg N/L (estimated based on the dissolved N₂O concentrations during daytime shown in Fig. 2 and the N₂O dynamics shown in Fig. 1), it was estimated that approximately 13.6 kg N/day of N₂O produced in the anoxic zone in the 2nd Step would flow into the aerobic zone. By assuming that the full amount was stripped out in the aerobic zone, the anoxic zone's contribution to the overall N₂O emission in the second Step would be 27% (13.6 kg N/day ÷ 49.8 N/day, 49.8 N/day is the average daily N₂O emission from the second step, as detailed in Table 2). This represents an upper limit of the anoxic zone contribution as some of the N₂O washed into the aerobic zone could potentially be reduced to N₂ by denitrifiers. Our analysis showed that the AOB were likely to be the primary contributors (>73%) to the high N₂O emission in the 2nd Step, which exceeded the AOB contribution in the 1st Step.

As shown in Table 2, the average daily N₂O emission from the 2nd Step was 49.8 kg N/day. Even when assuming all of the N₂O accumulated in the anoxic zone was stripped (13.6 kg N/day) the N₂O produced in the aerobic zone was 36.2 kg N/day (49.8 kg N/day - 13.6 kg N/day). This amount, which is likely to be highly conservative, was much higher than the N₂O emitted in the 1st Step (12.5 kg N/day). Therefore, the generation of N₂O by AOB activity in the 2nd Step was much higher than that in the 1st Step. Previous studies have shown that the biomass specific N₂O production rate increases as the ammonia oxidation rate increases³¹. This was shown to be true for both the hydroxylamine oxidation pathway and the AOB denitrification pathway³². These findings suggest that AOB tend to produce more N₂O at higher ammonia oxidation rates. In this study, the MLVSS concentration in the 2nd step was around 40% lower than that in the first step because of the dilution effect provided by influent from the 2nd step. The biomass specific nitrogen and COD loading rate to the 1st step were 0.047 kgN/(kgVSS × day) and 0.36 kgCOD/(kgVSS × day), in comparison to 0.065 kgN/(kgVSS × day) and 0.51 kgCOD/(kgVSS × day), respectively to the 2nd step. This led to a higher F/M (food to microorganism) ratio in the 2nd step and hence, a higher biomass specific ammonia oxidation rate, which favoured higher N₂O production.

One potential mitigation strategy could be to evenly divide the RAS into anoxic zones of both steps (currently RAS is returned only to the 1st step). In doing so, the MLVSS concentration in the 2nd step would increase, resulting in a lower F/M ratio which may reduce N₂O production. However, for this scenario N₂O production in the 1st step is expected to increase, however to a lesser extent, leading to a reduction in the overall N₂O emission from the system.

Material and Methods

Process scheme of the full-scale plug-flow step-feed activated sludge reactor. The ASR used for this case study employed a plug-flow step-feed configuration for biological nitrogen and carbon removal from domestic wastewater, with a design capacity of 50 ML/day. The reactor has a working volume of 21,205 m³, with a designed hydraulic retention time (HRT) of 12 h and aerobic sludge retention time (SRT) of 8 days (total SRT of 12 days).

A simplified process flow diagram of the reactor studied is shown in Fig. 4. The plug-flow reactor consists of four paths, each with a volume of 5340 m³ (89 m × 12 m × 5 m). The influent feed is split, where 56% (27.3 ML/day) is fed at the beginning of the 1st step and 44% (22.7 ML/day) is fed in the 2nd step, forming a two-step configuration. The 1st step consists of Path 1 and Path 2 and the 2nd step consists of Path 3 and Path 4. Each step is comprised of an anoxic zone for denitrification (3000 m³ for the 1st step and 4440 m³ for the 2nd step) followed by an aerobic zone for nitrification. The 2nd step begins with an anoxic zone with a working volume of 4440 m³ (74 m × 12 m × 5 m) for denitrification, followed by a second aerated zone for nitrification. The mixed liquor from Path 2 enters Path 3, which is mixed with the influent fed to this path in the anoxic zone. The effluent exits the reactor at the end of Path 4. The RAS from the secondary clarifiers, with a calculated flow rate of 18.1 ML/day, is recycled to the beginning of the anoxic zone of Path 1. Aeration control is based on online DO measurement with DO probes installed in each step (Fig. 4), with the DO set-point fixed at around 1 mg/L.

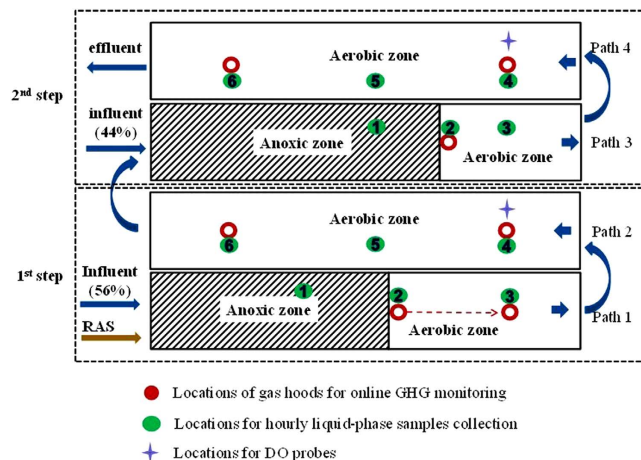


Figure 4. A simplified process flow diagram of the two-step plug-flow BNR reactor studied (the hood originally placed at Location 2 of the 1st step was moved to Location 3 after one-week monitoring, indicated by the arrow).

Gas-phase N_2O monitoring using gas hoods and on-line N_2O analysers. Multiple sampling locations were chosen in this study to investigate the spatial variation in N_2O emissions from different paths of the two-step plug-flow BNR reactor. The locations of the gas hoods used to collect the gas-phase N_2O concentration and gas flow data are as indicated in Fig. 4. These sampling points were specifically chosen to cover the beginning (Locations 2 and 3 of the 1st step, Location 2 of the 2nd step), the middle (Location 4 of each step) and the end (Location 6 of each step) of the aerobic zones. The gas hoods were not placed within the anoxic zones since there was no measurable gas flow here and previous studies have shown that N_2O fluxes from un-aerated zones are negligible¹⁰.

The on-line gas-phase N_2O monitoring was conducted over a seven week period. Three gas hoods were designed and anchored along the aerated zone to allow continuous online emission monitoring. During the first sampling week, the three hoods were placed at Location 2, Location 4 and Location 6 of the 1st step. In the second to the fourth sampling week, the hood originally placed at Location 2 was moved along the reactor to Location 3 of the 1st step, while the other two hoods remained at their same location. Between the fifth to the seventh sampling weeks, the three hoods were moved to the 2nd step, located at Locations 2, 4 and 6.

The three off-gas hoods were modified from plastic commercial hopper tanks. The wall of the hopper tank was shortened to approximately 280 mm, giving a total height of 540 mm (shown in Figure S2 in Supplementary Content). The bottom diameter was 530 mm and covered an area of 0.22 m². The hoods were lowered to allow a minimum depth of 100–150 mm into the water column, resulting in a maximum permissible gas pressure within the hoods of 1.0–1.5 kPa (to keep the wall of hoods submerged). Each of the plastic hopper hoods were attached with a high-density polystyrene skirt to ensure that they floated and were fixed in position using nylon rope secured to three anchor points.

The off-gas collected from each of the three gas hoods were transferred to a central off-gas monitoring unit, via 50mm diameter polyethylene gas tubing to allow continuous emission monitoring. A detailed description of the off-gas collection and monitoring unit is provided in Fig. 5. Once the off-gas from each of the hoods reached the monitoring unit, gas temperature, pressure and flow rate were measured and recorded in real-time. After the flow meter (Landis + Gyr, mode 750), a small portion of the gas (4 L/min) was diverted and pumped to the gas conditioning unit (Horiba VS3002) and analyzer (Horiba VA3000) via an internal air pump situated within the Horiba analyzer. The excess off-gas (20–100 L/min) was continuously exhausted from the outlet of the flow meter. As the analyzer can only measure one gas stream at a time, a Siemens Programmable Logic Controller (PLC) was used to control the cyclic opening and closing of solenoid valves to direct the gas captured from the individual hoods to the analyser at 6 minute intervals. N_2O concentration (in ppmv) temperature, flow rate and pressure were logged at two minute intervals. The gas analyser had a N_2O measurement range of 0 to 500 ppmv, with a detection limit of 2 ppmv at an accuracy of 1% of the scale. The analyser was serviced and calibrated on-site, according to manufacturer's instructions, using compressed air and 450 ppmv N_2O gas standard (Air Liquide Australia). In addition, other online data recorded by the plant operator, including the influent flow rate, aeration flow rate and DO concentrations were also collected.

Liquid phase measurements through off-line sampling. The purpose of the grab sampling campaign was to collect liquid-phase N_2O , as well as NH_4^+-N , $NO_3^- -N$, and $NO_2^- -N$ data to gain further insight into the N_2O production at different locations along the reactor. Hourly grab samples (from 8 am to 3 pm) were manually taken from multiple sampling locations shown in Fig. 4, for wastewater and mixed liquor composition analysis (more details in Table 3). These sampling points covered influent, anoxic zone (Location 1) and different locations along the aerobic zones (Location 2 to Location 6). Samples were analyzed for dissolved N_2O , NH_4^+-N , $NO_3^- -N$, and $NO_2^- -N$. The pH, temperature and DO were also measured hourly at these locations using a portable DO/pH/T meter (YSI Professional Plus, United States).

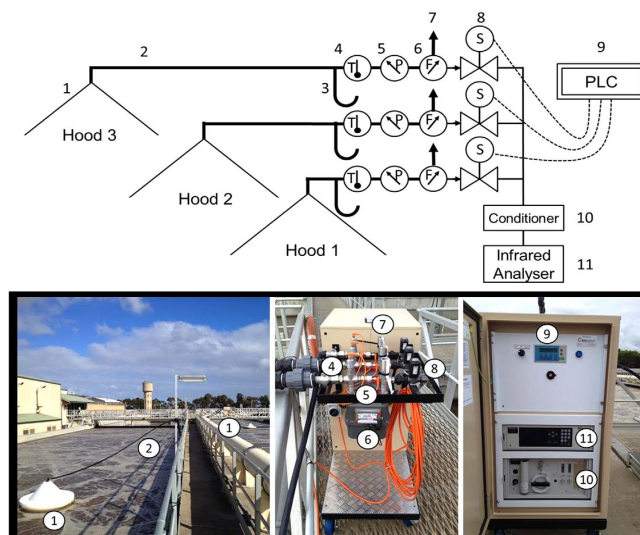


Figure 5. The monitoring system: (a) line diagram and (b) photograph of the set-up. (1) gas-hoods positioned along the aeration zone; (2) polyethylene gas tubing; (3) condensation moisture trap; (4) temperature sensor; (5) pressure sensor; (6) flow meter; (7) excess gas exhaust; (8) solenoid gas valve for multiple hood gas sampling; (9) programmable logic controller to control solenoid gas valves for gas sampling from each hood; (10) gas sample conditioning system; (11) infrared N_2O , CH_4 and O_2 gas analyzer.

Monitoring period	Hood location	Liquid phase sampling locations	Liquid phase sampling day
Week 1	the 1 st step: Locations 2, 4 & 6	None	None
Week 2 – Week 4	the 1 st step: Locations 3, 4 & 6	the 1 st step: influent, Locations 1, 2, 3, 4, 5 & 6	Week 4: on Tuesday and Wednesday
Week 5 – Week 7	the 2 nd step: Locations 3, 4 & 6	the 2 nd step: influent, Locations 1, 2, 3, 4, 5 & 6	Week 5: on Tuesday and Thursday

Table 3. On-line monitoring and offline sampling program.

In addition, 24 h composite samples were taken from the influent and effluent using refrigerated automatic samples for the measurement of TCOD, TKN, NH_4^+-N , $NO_3^- -N$ and $NO_2^- -N$.

Chemical analysis. The collected liquid samples were immediately filtered with 0.45 mm disposable sterile filters (Millipore, Millex GP) and were subsequently injected into freshly vacuumed Labco Exetainers to allow equilibration of gas and liquid phases. The N_2O concentrations in the gas phase of the tube were measured using a Shimadzu GC-9A gas chromatograph equipped with a micro-electron capture detector (ECD) and a flame ionization detector (FID), respectively. Each Labco Exetainer tube was weighed before and after sampling to determine the sample volume collected. This volume, along with the known volume of the Exetainers, enables the dissolved N_2O concentration contained in the original wastewater sample to be calculated¹⁵. The detection limit of the liquid phase N_2O concentration is 4.5×10^{-5} mg N/L. The filtered samples were also analysed for the NH_4^+ , NO_3^- and NO_2^- concentrations using Lachat QuickChem8000 Flow Injection Analyser (Lachat Instrument, Milwaukee, USA). Mixed liquor suspend solid (MLSS) and volatile solids (MLVSS) were measured in triplicates according to the Standard Methods³³. TCOD and TKN in samples collected were analysed according to Standard Methods³³.

Calculation of N_2O emission. The N_2O fluxes were calculated based on the online monitoring results of the gas-phase N_2O concentration, gas flow rate and temperature. The data collected by the three hoods in each step were all considered. The hood located at Location 3 of the 1st step and Location 2 of the 2nd step was used to represent the first 30% surface area of the respective aeration basin. Similarly, the hood located at Location 4 of both steps was used to represent the middle 40% surface area, and the hood located at Location 6 of both steps was used to represent the last 30% surface area. Since there was no measurable gas flow from the anoxic zone, the gas hoods were not placed here. Due to the lack of active stripping, N_2O emission from non-aerated areas has been found to be negligible in previous studies, and N_2O accumulated at the anoxic zone has been found to be stripped in the aeration zone in previous studies¹⁰.

The net N_2O emitted from each hood covered area over a given a period of time (Δt) were calculated using Eq-1:

$$\text{N}_2\text{O Emitted} = \Sigma(C_{\text{N}_2\text{O-N, gas}} * Q_{\text{air}} * \Delta t) \quad (1)$$

where $C_{\text{N}_2\text{O-N, gas}}$ is the $\text{N}_2\text{O-N}$ concentration in the off-gas (mg $\text{N}_2\text{O-N/L}$); Q_{air} is the flow rate of the off-gas (L/hour); Δt is time interval by which the off-gas N_2O concentration was measured (one minute in this study). The unit of N_2O concentration in the off-gas was converted from ppmv (directly measured by the on-line analyzer) to mg $\text{N}_2\text{O-N/L}$, and corrected for temperature at the time of sampling.

References

1. IPCC. Climate Change 2007: The Physical Science Basis. Contribution of Working Group I to the Fourth Assessment Report of the Intergovernmental Panel on Climate Change [Solomon, S., D. Qin, M. Manning, Z. Chen, M. Marquis, K. B. Averyt, M. Tignor and H. L. Miller (eds.)]. Cambridge University Press, Cambridge, United Kingdom and New York, NY, USA (2007).
2. De Haas, D. & Hartley, K. Greenhouse gas emission from BNR plants: do we have the right focus? *Proceedings of EPA Workshop: Sewage Management: Risk Assessment and Triple Bottom Line*, 5–7 (2004).
3. Foley, J., De Haas, D., Yuan, Z. & Lant, P. Nitrous oxide generation in full-scale biological nutrient removal wastewater treatment plants. *Water Res* **44**, 831–844 (2010).
4. Ahn, J. H. *et al.* N_2O emissions from activated sludge processes, 2008–2009: results of a national monitoring survey in the united states. *Environ Sci Technol* **44**, 4505–4511 (2010).
5. Aboobakar, A. *et al.* Nitrous oxide emissions and dissolved oxygen profiling in a full-scale nitrifying activated sludge treatment plant. *Water Res* **47**, 524–534 (2013).
6. Kampschreur, M. J. *et al.* Dynamics of nitric oxide and nitrous oxide emission during full-scale reject water treatment. *Water Res* **42**, 812–826 (2008).
7. Rodriguez-Caballero, A., Aymerich, I., Poch, M. & Pijuan, M. Evaluation of process conditions triggering emissions of green-house gases from a biological wastewater treatment system. *Sci Total Environ* **19**, 384–391 (2014).
8. Kampschreur, M. J., Temmink, H., Kleerebezem, R., Jetten, M. S. M. & van Loosdrecht, M. C. M. Nitrous oxide emission during wastewater treatment. *Water Res* **43**, 4093–4103 (2009).
9. Law, Y. *et al.* Full scale monitoring of fugitive nitrous oxide and methane emissions from a wastewater treatment plant in Australia. *OzWater '12: Australia's National Water Conference and Exhibition* (2012).
10. Law, Y., Ye, L., Pan, Y. & Yuan, Z. Philosophical Transactions of the Royal Society of London: Biological Sciences. *Philos Trans R Soc Lond B Biol Sci* **367**, 1265–1277 (2012).
11. Ahn, J. H. *et al.* Spatial and temporal variability in atmospheric nitrous oxide generation and emission from full-scale biological nitrogen removal and non-BNR processes. *Water Environ Res* **82**, 2362–2372 (2010).
12. Tchobanoglous, G., Burton, F. & Stensel, H. D. *Wastewater engineering: treatment and reuse*. 4th edn, (Metcalf & Eddy, Inc., McGraw Hill Education 2003).
13. Yang, Q. *et al.* N_2O production during nitrogen removal via nitrite from domestic wastewater: main sources and control method. *Environ Sci Technol* **43**, 9400–9406, (2009).
14. Yu, R., Kampschreur, M. J., Loosdrecht, M. C. M. v. & Chandran, K. Mechanisms and specific directionality of autotrophic nitrous oxide and nitric oxide generation during transient anoxia. *Environ Sci Technol* (2010).
15. Ye, L., Ni, B.-J., Law, Y., Byers, C. & Yuan, Z. A novel methodology to quantify nitrous oxide emissions from full-scale wastewater treatment systems with surface aerators. *Water Res* **48**, 257–268 (2014).
16. Zhu, X. & Chen, Y. Reduction of N_2O and NO generation in anaerobic–aerobic (low dissolved oxygen) biological wastewater treatment process by using sludge alkaline fermentation liquid. *Environ Sci Technol* **45**, 2137–2143 (2011).
17. Tallec, G., Garnier, J., Billen, G. & Gossailles, M. Nitrous oxide emissions from denitrifying activated sludge of urban wastewater treatment plants, under anoxia and low oxygenation. *Bioresource Technol* **99**, 2200–2209 (2008).
18. Lu, H. & Chandran, K. Factors promoting emissions of nitrous oxide and nitric oxide from denitrifying sequencing batch reactors operated with methanol and ethanol as electron donors. *Biotechnol Bioeng* **106**, 390–398 (2010).
19. Law, Y., Lant, P. & Yuan, Z. The Confounding Effect of Nitrite on N_2O Production by an Enriched Ammonia-Oxidizing Culture. *Environ Sci Technol* **47**, 7186–7194 (2013).
20. Rodriguez-Caballero, A. & Pijuan, M. N_2O and NO emissions from a partial nitrification sequencing batch reactor: Exploring dynamics, sources and minimization mechanisms. *Water Res* **47**, 3131–3140 (2013).
21. Law, Y., Lant, P. & Yuan, Z. The effect of pH on N_2O production under aerobic conditions in a partial nitrification system. *Water Res* **45**, 5934–5944 (2011).
22. Pan, Y., Ye, L., Ni, B.-J. & Yuan, Z. Effect of pH on N_2O reduction and accumulation during denitrification by methanol utilizing denitrifiers. *Water Res* **46**, 4832–4840 (2012).
23. Daelman, M. R. J., Van Voorthuizen, E. M., Van Dongen, L. G. J. M., Volcke, E. I. P. & Van Loosdrecht, M. C. M. Methane and nitrous oxide emissions from municipal wastewater treatment - Results from a long-term study. *Water Sci Technol* **67**, 2350–2355 (2013).
24. Rodriguez-Caballero, A., Aymerich, I., Marques, R., Poch, M. & Pijuan, M. Minimizing N_2O emissions and carbon footprint on a full-scale activated sludge sequencing batch reactor. *Water Res* **71**, 1–10 (2015).
25. Lotti, T. *et al.* Pilot-scale evaluation of anammox-based mainstream nitrogen removal from municipal wastewater. *Environ Technol*, 1–11 (2014).
26. Wunderlin, P., Mohn, J., Joss, A., Emmenegger, L. & Siegrist, H. Mechanisms of N_2O production in biological wastewater treatment under nitrifying and denitrifying conditions. *Water Res* **46**, 1027–1037 (2012).
27. Kim, T. H. *et al.* Characteristics of N_2O release from fluidized media type BNR processes and identification of N_2O sources. *Desalination and Water Treatment* **28**, 378–384 (2011).
28. Desloover, J. *et al.* Floc-based sequential partial nitrification and anammox at full scale with contrasting N_2O emissions. *Water Res* **45**, 2811–2821 (2011).
29. Pijuan, M. *et al.* Effect of process parameters and operational mode on nitrous oxide emissions from a nitrification reactor treating reject wastewater. *Water Res* **49**, 23–33 (2014).
30. Zhou, Y., Pijuan, M., Zeng, R. J. & Yuan, Z. Free nitrous acid inhibition on nitrous oxide reduction by a denitrifying-enhanced biological phosphorus removal sludge. *Environ Sci Technol* **42**, 8260–8265 (2008).
31. Law, Y., Ni, B.-J., Lant, P. & Yuan, Z. N_2O production rate of an enriched ammonia-oxidising bacteria culture exponentially correlates to its ammonia oxidation rate. *Water Res* **46**, 3409–3419 (2012).
32. Peng, L., Ni, B. J., Erler, D., Ye, L. & Yuan, Z. The effect of dissolved oxygen on N_2O production by ammonia-oxidizing bacteria in an enriched nitrifying sludge. *Water Res* **66**, 12–21 (2014).
33. Rand, M., Greenberg, A. E. & Taras, M. J. *Standard methods for the examination of water and wastewater*. (Prepared and published jointly by American Public Health Association, American Water Works Association, and Water Pollution Control Federation. 1976).

Acknowledgements

This study was funded by the Australian Research Council, South Australian Water Corporation, Western Australia Water Corporation and Melbourne Water Corporation through project LP0991765. Dr Yuting PAN acknowledge the project 51508355 supported by National Natural Science Foundation of China. Dr Bing-Jie Ni and Dr Liu Ye acknowledge the support of the Australian Research Council Discovery Early Career Researcher Awards DE130100451 and DE150100393, respectively.

Author Contributions

Y.P., L.Y. and Z.Y. conceived and designed the experiments. Y.P., B.V.D.A., S.W. and K.R. performed the experiments. Y.P., B.N. and Z.Y. analysed the data. Y.P., B.V.D.A. and Z.Y. wrote the paper.

Additional Information

Supplementary information accompanies this paper at <http://www.nature.com/srep>

Competing financial interests: The authors declare no competing financial interests.

How to cite this article: Pan, Y. *et al.* Unravelling the spatial variation of nitrous oxide emissions from a step-feed plug-flow full scale wastewater treatment plant. *Sci. Rep.* **6**, 20792; doi: 10.1038/srep20792 (2016).



This work is licensed under a Creative Commons Attribution 4.0 International License. The images or other third party material in this article are included in the article's Creative Commons license, unless indicated otherwise in the credit line; if the material is not included under the Creative Commons license, users will need to obtain permission from the license holder to reproduce the material. To view a copy of this license, visit <http://creativecommons.org/licenses/by/4.0/>